STRUCTURAL SCIENCE
CRYSTAL ENGINEERING
MATERIALS

**Volume 75 (2019)**

**Supporting information for article:**

# Elucidation of correlated disorder in zeolite IM-18

**Xiaoge Wang, Yihan Shen, Rongli Liu, Xiaolong Liu, Cong Lin, Dier Shi, Yanping Chen, Fuhui Liao, Jianhua Lin and Junliang Sun**

## S1. Materials and Methods

### S1.1. Other characterization

SEM images were captured with a Hitachi S4800 microscope to observe the sample morphology. As-synthesized IM-18 samples were dissolved in $NH_4F/HNO_3$ solution and quantitatively diluted, and the content of Si and Ge was determined on an ESCALAB2000 analyser by the ICP method. Carbon, hydrogen and nitrogen elements were measured on Elementary Vario EL III micro-analyser. The thermal gravimetric analysis was performed on TGA Q50 V20.6 with a heating rate of 10°C/min from 40°C to 800°C in 30ml/min air atmosphere. The solid-state $^{13}C$ NMR spectrum was performed on Bruker AVANCE III 400 MHz NMR spectrometer at spinning rates of 5 kHz, with a frequency of 100.65 MHz and a contact time of 3.5 ms. A 4 mm Bruker probe was used. The liquid $^{13}C$ NMR spectrum was performed on Bruker AVANCE III 500 MHz with $CD_3OD$ as the solvent in 5 mm probe. The frequency was set as 125.77 MHz and delay time was set as 2s. $^{19}F$ MAS NMR was recorded on a Bruker AVANCE III 400 MHz spectrometer with spinning rates of 20 kHz.

### S1.2. Chemical formula determination

Inductively coupled plasma test showed Si/Ge ratio is 2.127 in as made IM-18. $^{13}C$ NMR spectrums of the as-made sample showed the intact protonated DMAP molecules were occluded in the zeolite. And the chemical shift change in IM-18 (135.5 ppm) relative to that in liquid $CD_3OD$ (148.1 ppm) was assigned to the protonation of nitrogen in the pyridine. In $^{19}F$ MAS NMR spectrum (Figure S4), signals near -9.7 ppm, -16.6 ppm and -19.9 ppm are all assigned to the $F^-$ ions occluded in d4r units but with different Si/Ge ratios. Strong signal at -9.7 ppm points that [4Si, 4Ge] are dominant in the d4r units, and Signal at -19.9 ppm is assigned to the [7Si, 1Ge](Liu *et al.*, 2012). Weak peak -16.6ppm is inferred as [n Si, (8-n)Ge] ($4 < n < 7$) in *d*4*r* sites. The thermal gravimetric analysis shows about 14% weight loss after heating as-made sample with air current to 800°C. CHN elements analysis shows there is about 12% weight for organic species. Occupancy refinement showed the Ge atoms mainly locate in *d*4*r* positions. Finally, chemical formula $(C_7H_{11}N_2)$ $FGe_{3.84}Si_{8.16}O_{24}$ was determined.

### S1.3. Structure determination

The IM-18 crystallizes in the space group *Imma* with $a$ = 14.9725(14) Å, $b$ = 5.2733(6) Å, $c$ = 17.0318(17) Å. The initial structure determination showed this structure has disordered *d*4*r* units. Detailed refinement demonstrated the existence of half-occupancy in disordered *d*4*r* sites. We got the average IM-18 structure with half-occupancy *d4r* units connected by the zigzag chain. The Si/Ge occupancy on *d*4*r* sites was refined to 0.552/0.448 and 0.936/0.064 in the zigzag chain (meaning almost

all T atoms are Si in zigzag chain sites). The $^{19}F$ NMR spectrum (Figure S4) shows the $F^-$ ions occluded in the *d*4*r* units and the $^{13}C$ NMR spectrum (Figure S3) shows the intact existence of the protonated DMAP occluded in zeolite IM-18. Residual electron density of the framework shows the protonated DMAP molecules half occupy the same sites for the d4r units. There are three T atoms in the asymmetric unit with the T1 atom (mainly occupied by Si) in *zigzag* chains and half occupied T2 and T3 atoms (mixed with Ge and Si) in the disordered *d*4*r* units. Fluorine ions are occluded in the *d*4*r* units and the protonated DMAP molecules half occupy the same sites as the *d*4*r* units. Crystal data and refinement details are given in Table S1, S2 and S3. CCDC 1857218 contains the supplementary crystallographic data for this paper. The data can be obtained free of charge from the Cambridge Crystallographic Data Centre via www.ccdc.cam.ac.uk/data_request/cif.

## S2. Figures

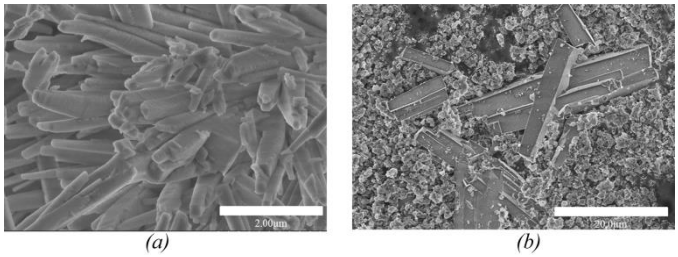


**Figure S1** The SEM pictures of *(a)* aggregated polycrystalline sample, and *(b)* the sample consisting of both the single crystals and polycrystalline particles.

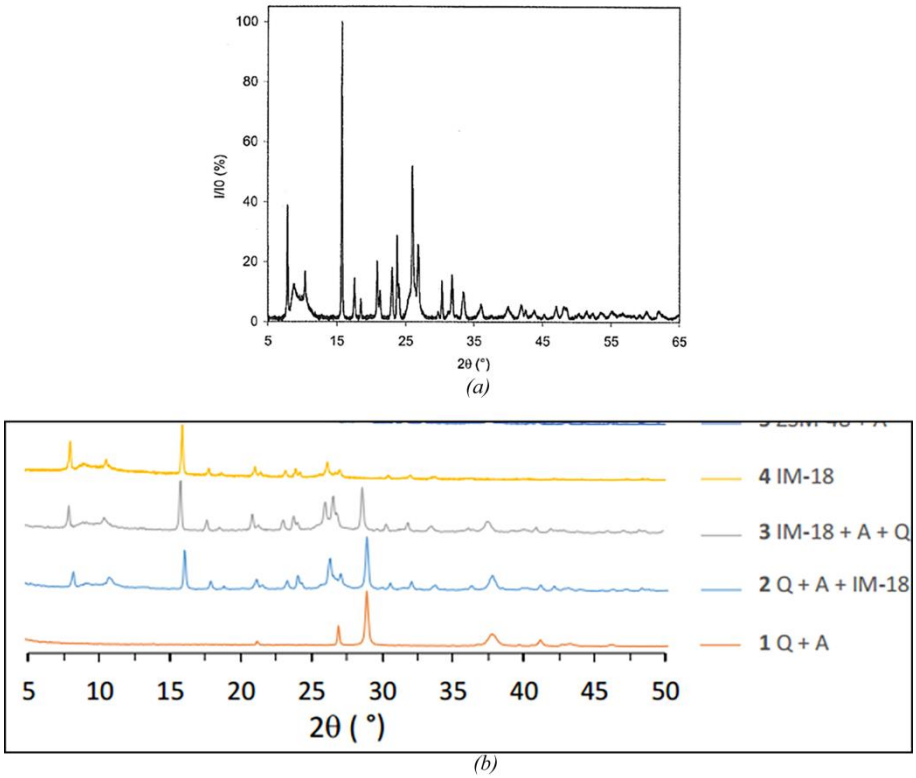


**Figure S2** *(a)* The PXRD pattern of the firstly reported IM-18 in the patent (Lorgouilloux *et al.*); and *(b)* the PXRD pattern of the sample (No.4 in Figure S2b) used for structure refinement in the work reported by J. L. Paillaud and X. Zou (Cichocka *et al.*, 2018). In the previous work, this picture was placed in the SI and the broad peaks were subtracted for the PXRD refinement.

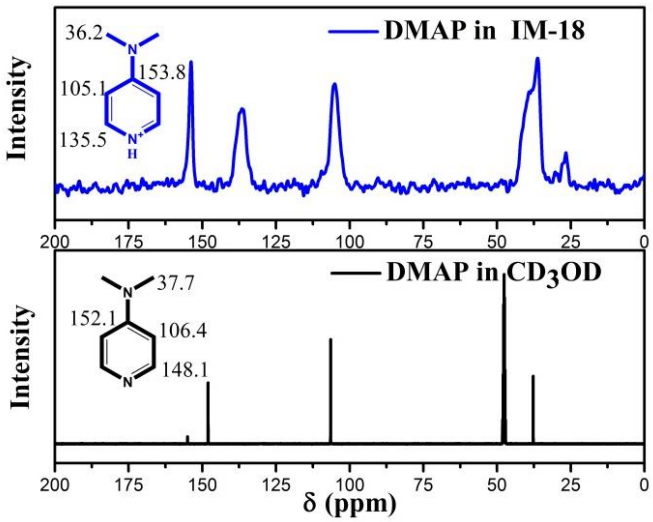


**Figure S3** $^{13}$C MAS NMR spectrums of DMAP dissolved in $CD_3OD$ and occluded in IM-18. There are four types of carbon atoms. The carbon atoms near the N atom in pyridine ring have the biggest change in IM-18 (135.5 ppm) relative to that in liquid $CD_3OD$ (148.1 ppm). Protonation of nitrogen in the pyridine group enhances the difference of chemical shift.

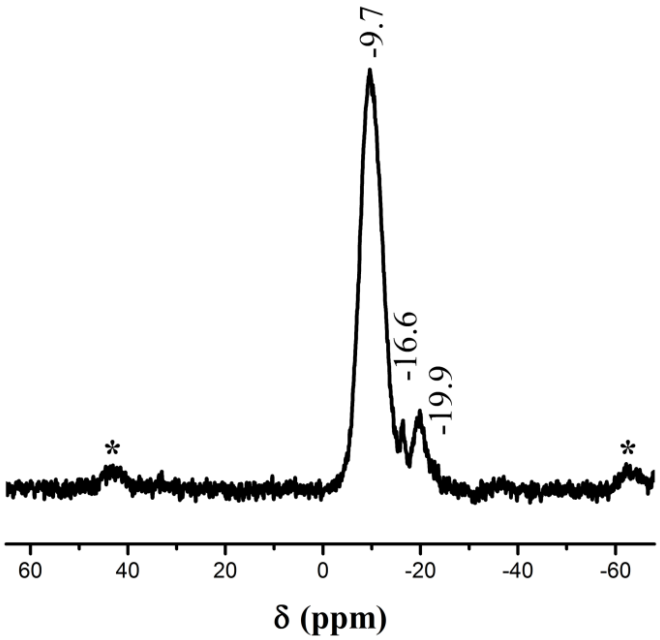


**Figure S4** $^{19}$F MAS NMR spectrum of as-made IM-18. The strong signal at-9.7 ppm shows that the [4Si, 4Ge] are dominant in *d4r* units. Signal at -19.9 ppm is assigned to the [7Si, 1Ge]. Weak peak -16.6ppm is inferred as [*n* Si, (8-*n* )Ge] ( 4 < n < 7) in *d4r* sites. (Wang *et al.*, 2003; Liu *et al.*, 2012) Spinning sidebands are marked by asterisks.

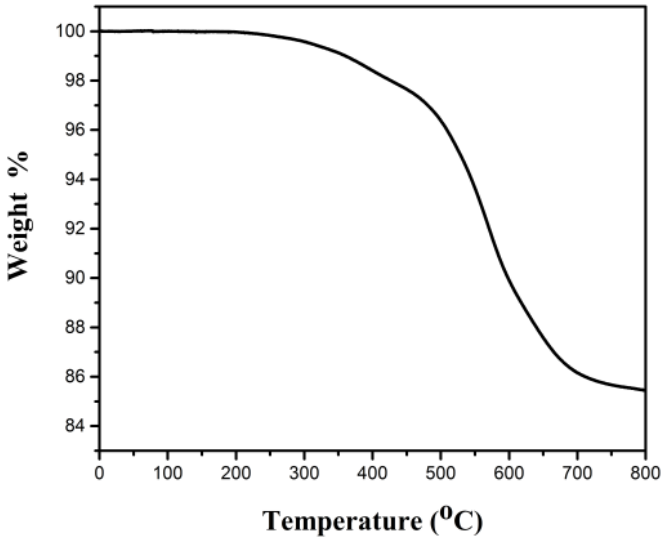


**Figure S5** TG curve of as made IM-18. The main weight loss between 200°C and 800°C is regarded as the removal of OSDAs.

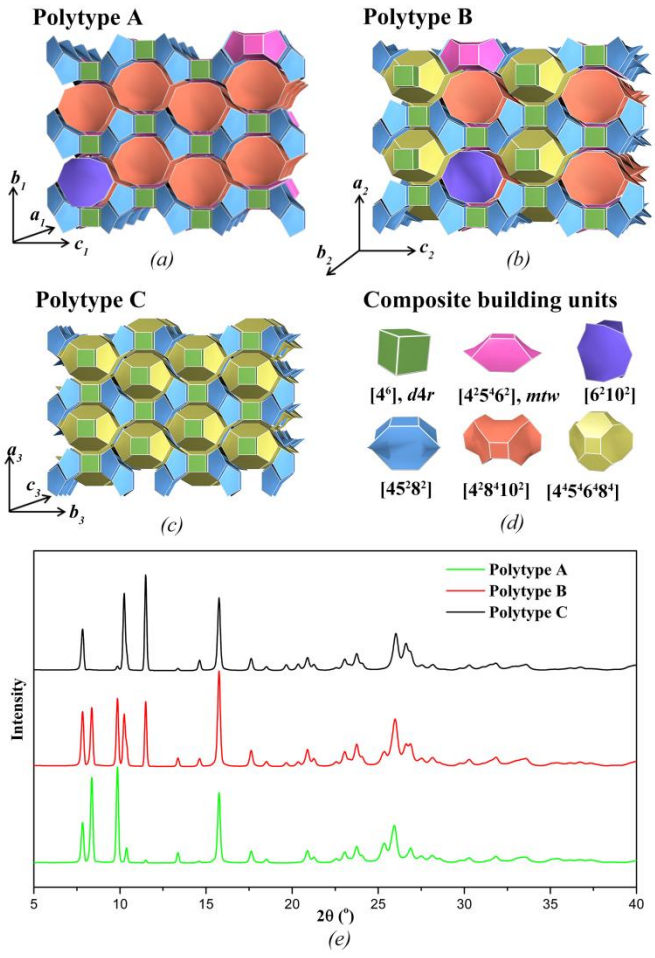


**Figure S6** The topologies of the simplest ordered structures of IM-18—*(a)* Polytype A, *(b)* Polytype B, and *(c)* Polytype C illustrated by the tile mode; *(d)* the composite building units for structure construction illustrated by the tile mode; (e) the simulated PXRD patterns of the three polytypes. The

topological analysis and visualization of all the tiles operated by the software TOPOS and program 3dt (Oldaf. Delgado-Friedrichs, 2003).

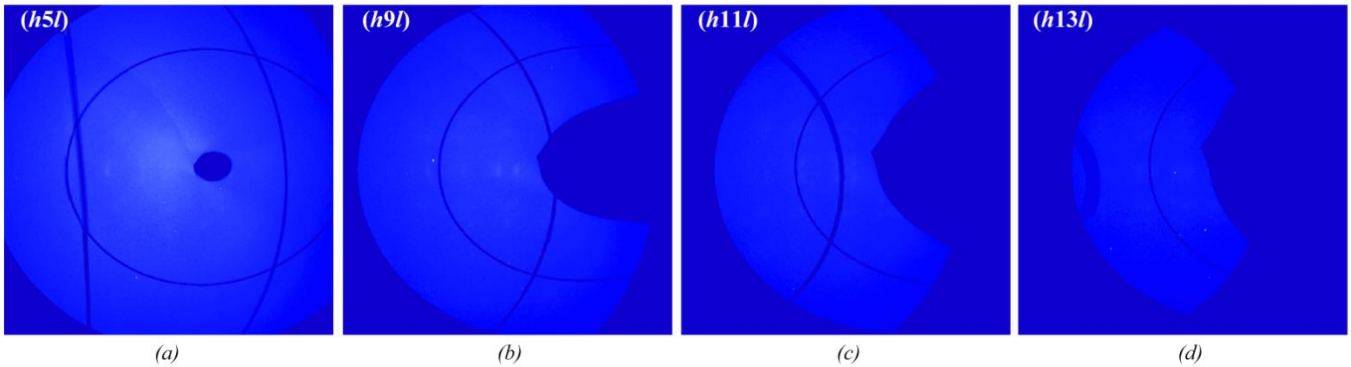


**Figure S7** The reconstructing procession photographs of the (*h*5*l*), (*h*9*l*), (*h*11*l*) and (*h*13*l*) planes from the SXRD data.

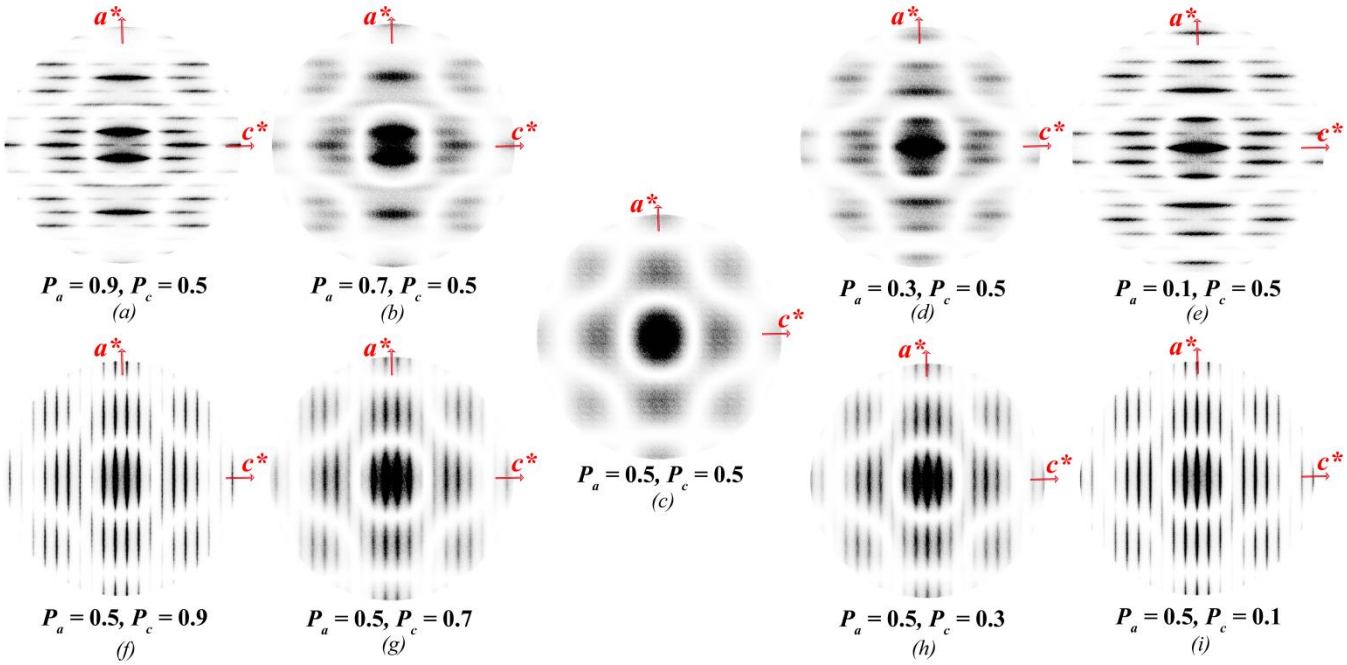


**Figure S8** The different diffuse scattering of (*h*3*l*) planes as the supercell models were constructed with the fixed $P_c$ = 0.5 but varying $P_a$, or fixed $P_a$ = 0.5 but varying $P_c$. The diffuse scattering is completely continuous for the highly disordered case with $P_a$ = 0.5 and $P_c$ = 0.5 as shown in *(c)*; the discrete level of the scattering would increase as the probability value gets close to 1 or 0 as shown in *(a)*, *(e)*, *(f)* and *(i)*; the intensity of the midpoint on the pattern tends to vanish when the probability (no matter $P_a$ or $P_c$) value gets close to 1 as shown in *(a)* and *(f)*, and its diffraction signal tends to be high as the probability value approaches 0 as shown in *(e)* and *(i)*.

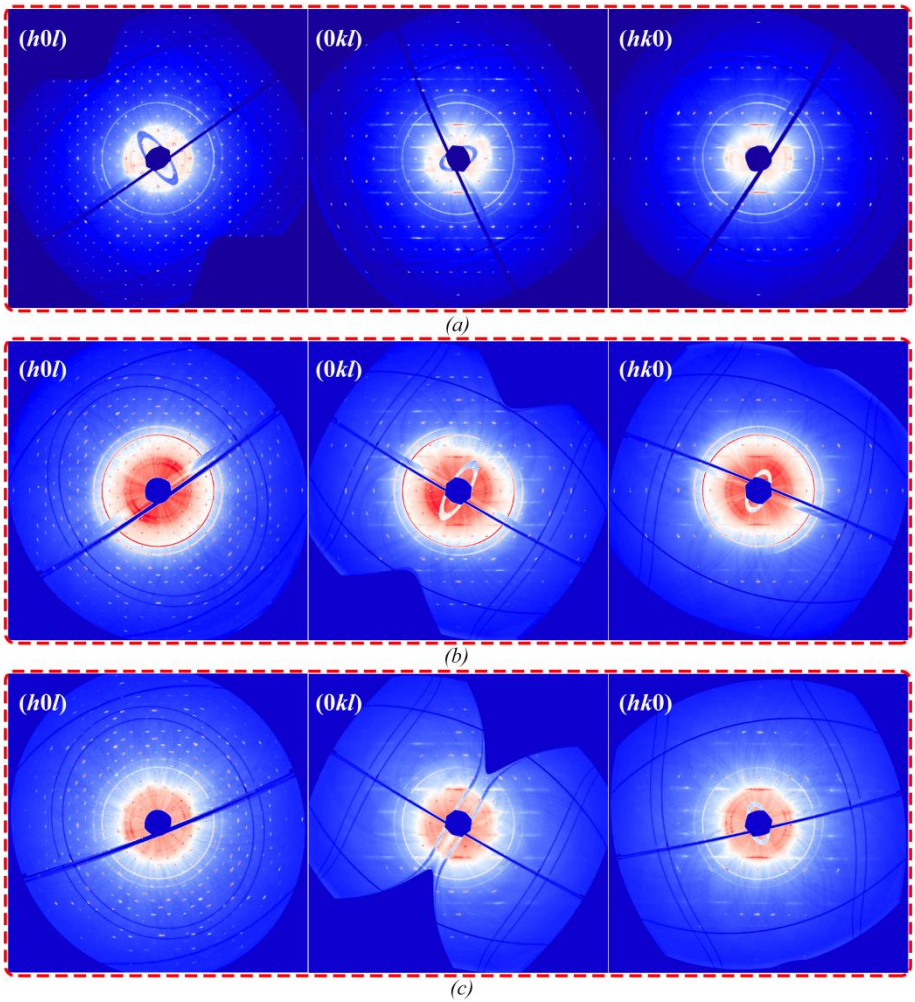


**Figure S9** *(a)*, *(b)* and *(c)* show the observed SXRD patterns of (*h*0*l*), (0*kl*) and (*hk*0) planes of three different single crystals. The diffraction rings (red or white rings) shown in the patterns are the diffraction of metal capillary outside of the synchrotron X-ray beam due to the poor collimation of the inner wall of the capillary.

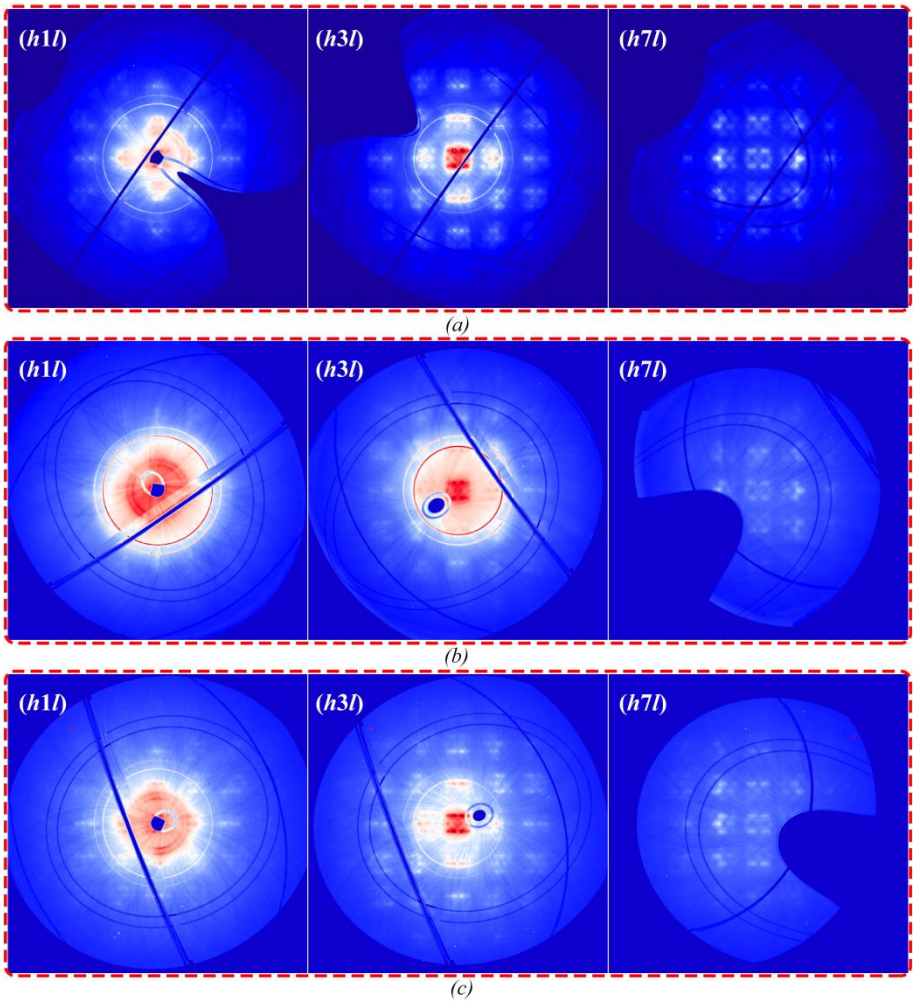


**Figure S10** *(a)*, *(b)* and *(c)* show the observed SXRD patterns of (*h*1*l*), (*h*3*l*) and (*h*7*l*) planes of three different single crystals. The diffraction rings (red or white rings) shown in the patterns are the diffraction of metal capillary outside of the synchrotron X-ray beam due to the poor collimation of the inner wall of the capillary.

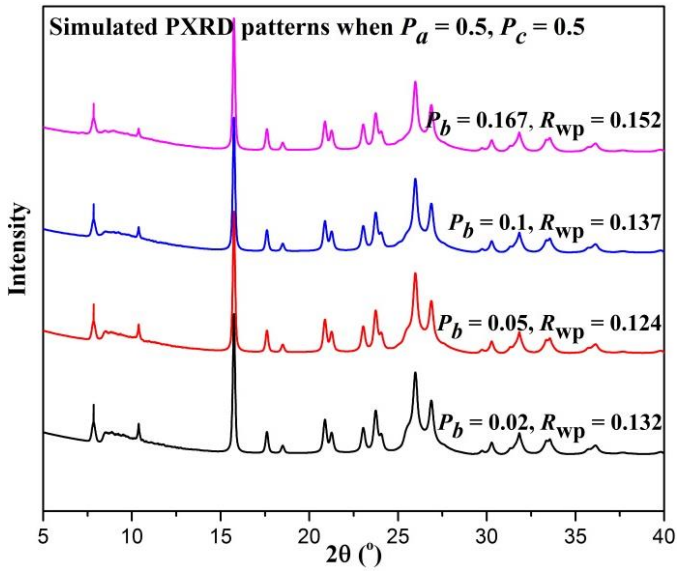


**Figure S11** Simulated PXRD patterns of the supercell models with the 2D disorder in interrupted structure. For the 2D disorder, supercell models with $P_a$=0.5 and $P_c$=0.5 were constructed according to the previous simulation results. For the defects inside the *d*4*r* columns, different $P_b$ values were used to index the defect degree to calculate the best-fitting pattern.

## S3. Tables

**Table S1** Sites and occupancies of the atoms in the average IM-18 structure.

| Atom | *x* | *y* | *z* | Occupancy |
|---|---|---|---|---|
| Ge1(T1) | 0.72466(5) | 0.7500 | 0.55026(4) | 0.064 |
| Si1 (T1) | 0.72466(5) | 0.7500 | 0.55026(4) | 0.936 |
| Ge2 (T2) | 0.60355(4) | 0.54692(12) | 0.87030(3) | 0.2675 |
| Si2 (T2) | 0.60355(4) | 0.54692(12) | 0.87030(3) | 0.2325 |
| Ge3 (T3) | 0.60509(4) | 0.54709(13) | 0.68732(4) | 0.1806 |
| Si3 (T3) | 0.60509(4) | 0.54709(13) | 0.68732(4) | 0.3194 |
| O1 | 0.69908(18) | 0.5000 | 0.5000 | 1.0 |
| O2 | 0.83132(15) | 0.7500 | 0.57114(15) | 1.0 |
| O3 | 0.66640(16) | 0.7500 | 0.63052(14) | 1.0 |
| O4 | 0.6417(4) | 0.2500 | 0.6732(3) | 0.5 |
| O5 | 0.5000 | 0.5829(10) | 0.6566(3) | 0.5 |
| O6 | 0.6437(3) | 0.2500 | 0.8873(3) | 0.5 |
| O7 | 0.5000 | 0.6102(10) | 0.9054(3) | 0.5 |
| O8 | 0.6220(2) | 0.6529(7) | 0.77793(19) | 0.5 |
| F1 | 0.5000 | 0.2500 | 0.7878(3) | 0.5 |
| N01 | -0.0629 | 0.2500 | 0.5827(3) | 0.25 |
| C01 | 0.0266 | 0.2500 | 0.5883(3) | 0.25 |
| C02 | 0.0735 | 0.2500 | 0.6572(3) | 0.25 |
| C03 | 0.0274 | 0.2500 | 0.7284(3) | 0.25 |
| C04 | -0.0659 | 0.2500 | 0.7228(3) | 0.25 |
| C05 | -0.1054 | 0.2500 | 0.6506(3) | 0.25 |
| N02 | 0.0705 | 0.2500 | 0.7983(3) | 0.25 |
| C06 | 0.1662 | 0.2500 | 0.8016(3) | 025 |
| C07 | 0.0207 | 0.2696 | 0.8708(3) | 0.125 |
| H00 | -0.0935 | 0.2500 | 0.5235 | 0.25 |
| H01 | 0.0599 | 0.2500 | 0.5366 | 0.25 |
| H02 | 0.1367 | 0.2500 | 0.6551 | 0.25 |
| H04 | -0.1023 | 0.2500 | 0.7695 | 0.25 |
| H05 | -0.1718 | 0.2500 | 0.6469 | 0.25 |
| H06A | 0.1936 | 0.3764 | 0.7659 | 0.125 |
| H06B | 0.1859 | 0.2500 | 0.8563 | 0.25 |
| H06C | 0.1856 | 0.0767 | 0.7806 | 0.125 |
| H07A | 0.0637 | 0.2989 | 0.9134 | 0.125 |

| | | | | |
|---|---|---|---|---|
| H07B | -0.0260 | 0.4082 | 0.8700 | 0.125 |
| H07C | -0.0120 | 0.1077 | 0.8815 | 0.125 |

**Table S2** T-O distances (Å) in average IM-18 structure.

T-O distances range from 1.617 Å to 1.7585 Å.

| Atom1 | Atom2 | distances(Å) | Atom1 | Atom2 | distances(Å) |
|---|---|---|---|---|---|
| (Si1, Ge1) | O1 | 1.6178(8) | (Si1, Ge1) | O2 | 1.636(2) |
| (Si1, Ge1) | O3 | 1.622(2) | (Si3, Ge3) | O8 | 1.660(3) |
| (Si2, Ge2) | O8 | 1.692(3) | (Si3, Ge3) | O5 | 1.6688(18) |
| (Si2, Ge2) | O7 | 1.695(2) | (Si3, Ge3) | O4 | 1.6773(19) |
| (Si2, Ge2) | O6 | 1.702(2) | (Si3, Ge3) | O3 | 1.7098(19) |
| (Si2, Ge2) | O2 | 1.7585(19) | | | |

**Table S3** O-T-O and T-O-T angles (º) in average IM-18 structure.

O-T-O angles range from 100.8º to 116.4º, T-O-T angles range from 131.65º to 152.62º.

| Atom1 | Atom2 | Atom3 | Angles(°) | Atom1 | Atom2 | Atom3 | Angles(°) |
|---|---|---|---|---|---|---|---|
| O1 | (Si1, Ge1) | O1 | 109.15(7) | O2 | (Si1, Ge1) | O3 | 109.99(13) |
| O1 | (Si1, Ge1) | O2 | 110.25(10) | O1 | (Si1, Ge1) | O3 | 108.58(8) |
| O8 | (Si2, Ge2) | O7 | 114.3(2) | O8 | (Si3, Ge3) | O5 | 113.4(2) |
| O8 | (Si2, Ge2) | O6 | 113.8(2) | O8 | (Si3, Ge3) | O4 | 113.4(2) |
| O8 | (Si2, Ge2) | O2 | 103.62(15) | O8 | (Si3, Ge3) | O3 | 103.51(15) |
| O7 | (Si2, Ge2) | O6 | 116.4(2) | O5 | (Si3, Ge3) | O4 | 111.7(3) |
| O7 | (Si2, Ge2) | O2 | 100.81(18) | O5 | (Si3, Ge3) | O3 | 104.95(19) |
| O6 | (Si2, Ge2) | O2 | 105.53(17) | O4 | (Si3, Ge3) | O3 | 109.13(18) |
| Si1 | O1 | Si1 | 152.62(19) | (Si3, Ge3) | O5 | (Si3, Ge3) | 141.1(3) |
| Si1 | O2 | (Si2, Ge2) | 131.65(10) | (Si2, Ge2) | O6 | (Si2, Ge2) | 133.8(3) |
| Si1 | O3 | (Si3, Ge3) | 139.98(7) | (Si2, Ge2) | O7 | (Si2, Ge2) | 132.4(3) |
| (Si3, Ge3) | O4 | (Si3, Ge3) | 138.1(3) | (Si2, Ge2) | O8 | (Si3, Ge3) | 149.4(2) |

**Table S4** Sites and occupancies of T and oxygen atoms in Polytype A.

Polytype A: space group *Pmna*, *a*=14.9725, *b*=10.5466, *c*=17.0318 Å.

| Atom | *x* | *y* | *z* | Occupancy |
|---|---|---|---|---|
| T1 | 0.39645 | 0.47654 | 0.87030 | 1.0 |
| T2 | 0.39491 | 0.47646 | 0.68732 | 1.0 |
| T3 | 0.89645 | 0.22654 | 0.37030 | 1.0 |
| T4 | 0.89491 | 0.22645 | 0.18732 | 1.0 |

| | | | | |
|---|---|---|---|---|
| T5 | 0.72466 | 0.37500 | 0.55026 | 1.0 |
| T6 | 0.22466 | 0.12500 | 0.05026 | 1.0 |
| O1 | 0.37800 | 0.42355 | 0.77793 | 1.0 |
| O2 | 0.87800 | 0.17355 | 0.27793 | 1.0 |
| O3 | 0.83132 | 0.37500 | 0.57114 | 1.0 |
| O4 | 0.66640 | 0.37500 | 0.63052 | 1.0 |
| O5 | 0.33132 | 0.12500 | 0.07114 | 1.0 |
| O6 | 0.16640 | 0.12500 | 0.13052 | 1.0 |
| O7 | 0.69908 | 0.25000 | 0.50000 | 1.0 |
| O8 | 0.14170 | 0.37500 | 0.17320 | 1.0 |
| O9 | 0.14370 | 0.37500 | 0.38730 | 1.0 |
| O10 | 0.19908 | 0.00000 | 0.00000 | 0.5 |
| O11 | 0.50000 | 0.45855 | 0.65660 | 0.5 |
| O12 | 0.50000 | 0.44490 | 0.90540 | 0.5 |
| O13 | 0.00000 | 0.20855 | 0.15660 | 0.5 |
| O14 | 0.00000 | 0.19490 | 0.40540 | 0.5 |
| O15 | 0.19908 | 0.50000 | 0.00000 | 0.5 |

**Table S5** Sites and occupancies of T and oxygen atoms in Polytype B.

Polytype B: space group $P2_1/m$, $a$=10.5466, $b$= 14.9725, $c$=17.0318 Å.

| Atom | *x* | *y* | *z* | Occupancy |
|---|---|---|---|---|
| T1 | 0.60154 | 0.14645 | 0.37970 | 1.0 |
| T2 | 0.60145 | 0.14491 | 0.56268 | 1.0 |
| T3 | 0.89846 | 0.35355 | 0.37970 | 1.0 |
| T4 | 0.89855 | 0.35509 | 0.56268 | 1.0 |
| T5 | 0.35154 | 0.64645 | 0.87970 | 1.0 |
| T6 | 0.35145 | 0.64491 | 0.06268 | 1.0 |
| T7 | 0.35154 | 0.35355 | 0.12030 | 1.0 |
| T8 | 0.35145 | 0.35509 | 0.93732 | 1.0 |
| T9 | 0.00000 | 0.47466 | 0.69974 | 1.0 |
| T10 | 0.50000 | 0.47466 | 0.69974 | 1.0 |
| T11 | 0.25000 | 0.97466 | 0.19974 | 1.0 |
| T12 | 0.25000 | 0.02534 | 0.80026 | 1.0 |
| O1 | 0.54855 | 0.12800 | 0.47207 | 1.0 |
| O2 | 0.29855 | 0.62800 | 0.97207 | 1.0 |
| O3 | 0.29855 | 0.37200 | 0.02793 | 1.0 |

| | | | | |
|---|---|---|---|---|
| O4 | 0.50000 | 0.58132 | 0.67886 | 1.0 |
| O5 | 0.50000 | 0.41640 | 0.61948 | 1.0 |
| O6 | 0.25000 | 0.08132 | 0.17886 | 1.0 |
| O7 | 0.25000 | 0.91640 | 0.11948 | 1.0 |
| O8 | 0.25000 | 0.91868 | 0.82114 | 1.0 |
| O9 | 0.25000 | 0.08360 | 0.88052 | 1.0 |
| O10 | 0.37500 | 0.44908 | 0.75000 | 1.0 |
| O11 | 0.12500 | 0.94908 | 0.25000 | 1.0 |
| O12 | 0.12500 | 0.05092 | 0.75000 | 1.0 |
| O13 | 0.37500 | 0.55092 | 0.25000 | 1.0 |
| O14 | 0.50000 | 0.89170 | 0.07680 | 1.0 |
| O15 | 0.50000 | 0.89370 | 0.86270 | 1.0 |
| O16 | 0.25000 | 0.60830 | 0.42320 | 1.0 |
| O17 | 0.25000 | 0.60630 | 0.63730 | 1.0 |
| O18 | 0.95145 | 0.37200 | 0.47207 | 1.0 |
| O19 | 0.00000 | 0.58132 | 0.67886 | 1.0 |
| O20 | 0.00000 | 0.41640 | 0.61948 | 1.0 |
| O21 | 0.58355 | 0.25000 | 0.59340 | 0.5 |
| O22 | 0.56990 | 0.25000 | 0.34460 | 0.5 |
| O23 | 0.33355 | 0.25000 | 0.90660 | 0.5 |
| O24 | 0.31990 | 0.25000 | 0.15540 | 0.5 |
| O25 | 0.91645 | 0.25000 | 0.59340 | 0.5 |
| O26 | 0.93010 | 0.25000 | 0.34460 | 0.5 |
| O27 | 0.33355 | 0.75000 | 0.09340 | 0.5 |
| O28 | 0.31990 | 0.75000 | 0.84460 | 0.5 |

**Table S6** Sites and occupancies of T and oxygen atoms in Polytype C.

Polytype C: space group *Pnnm*, *a*=10.5466, *b*=17.0318, *c* =14.9725Å.

| Atom | *x* | *y* | *z* | Occupancy |
|---|---|---|---|---|
| T1 | -0.02346 | 0.37030 | 0.39645 | 1.0 |
| T2 | -0.02355 | 0.18732 | 0.39491 | 1.0 |
| T3 | -0.27346 | 0.62970 | -0.39645 | 1.0 |
| T4 | -0.27354 | 0.81268 | -0.39491 | 1.0 |
| T5 | -0.37500 | 0.55026 | -0.22466 | 1.0 |
| T6 | -0.12500 | 0.44974 | 0.22466 | 1.0 |
| O1 | -0.07645 | 0.27793 | 0.37800 | 1.0 |

| | | | | |
|---|---|---|---|---|
| O2 | -0.32645 | 0.72207 | -0.37800 | 1.0 |
| O3 | -0.37500 | 0.57114 | -0.33132 | 1.0 |
| O4 | -0.37500 | 0.63052 | -0.16640 | 1.0 |
| O5 | -0.12500 | 0.42886 | 0.33132 | 1.0 |
| O6 | -0.12500 | 0.36948 | 0.16640 | 1.0 |
| O7 | -0.25000 | 0.50000 | -0.19908 | 1.0 |
| O8 | -0.37500 | 0.32680 | 0.14170 | 1.0 |
| O9 | -0.37500 | 0.11270 | 0.14370 | 1.0 |
| O10 | 0.00000 | 0.00000 | 0.30092 | 0.5 |
| O11 | 0.00000 | 0.50000 | 0.19908 | 0.5 |
| O12 | -0.04145 | 0.15660 | 0.50000 | 0.5 |
| O13 | -0.05510 | 0.40540 | 0.50000 | 0.5 |
| O14 | -0.29145 | 0.84340 | 0.50000 | 0.5 |
| O15 | -0.30510 | 0.59460 | 0.50000 | 0.5 |

**Table S7** Si and Ge elements analysis.

| ICP analysis | | | |
|---|---|---|---|
| | Si ($\mu$g/mL) | Ge ($\mu$g/mL) | Si/Ge ratio |
| Test | 1.5723 | 1.9117 | 2.127 |

**Table S8** C, H, and N elements analysis.

| CHN analysis | | | |
|---|---|---|---|
| | C (wt. %) | H (wt. %) | N (wt. %) |
| Test | 8.28 | 1.15 | 2.73 |